Physical and Chemical Characterization of Particles in the Upper Troposphere and Lower Stratosphere: Microanalysis of Aerosol Impactor Samples

NASA Final Report - Grant # NAG2-953

Patrick J. Sheridan, Principal Investigator
Research Associate/Research Scientist III
Cooperative Institute for Research in Environmental Sciences
Campus Box 449
University of Colorado
Boulder, CO 80309-0449

January 1999

Summary

NASA Grant No. NAG2-953 was to support the characterization of the aerosol in the upper troposphere and lower stratosphere (UT and LS) collected during the ASHOE/MAESA missions in 1994. Through a companion proposal, Professor J.C. Wilson's research group at the University of Denver was funded to measure the size distribution of aerosols in the 0.008 to 2 μm diameter range and to collect for us impactor samples of particles larger than about 0.02 μm. In the first year, we conducted laboratory studies related to particulate deposition patterns on our collection substrates, and have performed the analysis of many ASHOE/MAESA aerosol samples from 1994 using analytical electron microscopy (AEM). We have been building an "aerosol climatology" with these data that documents the types and relative abundances of particles observed at different latitudes and altitudes. The second year (and non-funded extension periods) saw continued analyses of impactor aerosol samples, including more ASHOE/MAESA samples, some northern hemisphere samples from the NASA SPADE program for comparison, and a few aerosol samples from the NASA STRAT program. A high-resolution field emission microscope was used for the analysis and re-analysis of a number of samples to determine if this instrument was superior in performance to our conventional electron microscope. In addition, some basic laboratory studies were conducted to determine the minimum detectable and analyzable particle size for different types of aerosols.

In all, 61 aerosol samples were analyzed, with a total of over 30,000 individual particle analyses. In all analyzed samples, sulfate particles comprised the major aerosol number fraction. It must be stressed that particles composed of more than one species, for example sulfate and organic carbon, were classified according to the major fraction. Thus, many of the particles classified as sulfate may have contained significant mass fractions of carbonaceous or other material. These particles for the most part did not show two physical phases, however. Nonsulfate particles were classified according to the physical and chemical characteristics of each particle, and were grouped into the major nonsulfate particle classes, including C-rich, crustal, metallic, and salts. Our UT and LS sample analyses indicate a maximum for crustal and C-rich particle abundance in the Northern Hemisphere upper troposphere, and a salt particle maximum in the Southern Hemisphere upper troposphere. Metallic particles are clearly more prevalent in the troposphere than in the stratosphere, but interhemispheric differences appear small.

Budget Details

Grant # NAG2-953 was for (1) developing the methodology to collect and analyze aerosol samples collected by the ER-2 aircraft using the University of Denver multiple-sample low-pressure impactor, (2) determining instrumental detection limits with our microanalysis systems, and (3) analyzing the upper tropospheric and lower stratospheric aerosol samples from the 1994 ASHOE/MAESA expedition.

The active period of the grant was 12/1/94 - 5/31/98 (including two 6-month non-funded extensions). The non-funded extensions were necessary primarily because of the substantial delay in bringing the new 300 keV field emission electron microscope on-line at the National Institute for Standards and Technology (NIST) in Gaithersburg, MD. This state-of-the-art instrument was not operational until August 1996, 21 months after the grant was made and significantly later than even the latest estimate from NIST. We therefore decided to use a conventional analytical electron microscope that we have used in previous NASA studies for our analyses. Instrument down-time for repairs and modifications and increased use of the older electron microscope were also contributing reasons for the extensions. Details regarding specific reasons for the delays and extensions were provided in our Continuation Proposal for Grant #NAG2-953, and the two funding extension request letters.

Introduction

In 1994, we collected atmospheric aerosol particles for subsequent electron microscope analysis using a sampler onboard the NASA ER-2 research aircraft. Our major objective was to characterize, both physically and chemically, the aerosol composition in the remote upper troposphere and lower stratosphere. By building what is essentially an extensive global aerosol climatology, we hope to be able to provide important data that will help to address some important secondary objectives. These include searching for the signal of aircraft impact in the atmosphere, characterizing particle surfaces as possible hosts of heterogeneous chemistry, characterizing aerosols that may serve as nuclei for clouds and contrails, studying regions of new particle formation, and studying stratosphere/troposphere exchange processes. This paper reports on the distribution and gradients of particle types found in a large latitude band over the Pacific Ocean.

Research Objectives

Before we can assess the impact to stratospheric chemistry of an *increased* aerosol burden, we must know what the present burden is, including the characteristics of the current (i.e., non-HSCT perturbed) aerosol in terms of microphysical parameters such as total particle number density and number-, surface area-, volume-, and mass-size distributions, chemical composition, physical phase and morphology. The research objectives were thus to gain a better knowledge on as many of these LS and UT aerosol characteristics as possible given the limited number of ASHOE/MAESA flights. Continuous *in situ* sensors on the ER-2 (condensation nucleus counter, CNC, and focused cavity aerosol spectrometer, FCAS) operated by the University of Denver measured the microphysical parameters, and impactor samples were collected for our subsequent

electron microscope (EM) studies of stratospheric particle composition, size, shape, physical state, and relative abundance. This Final Report presents our methods and findings from these activities.

Methods

The experimental methods used in this study have been described elsewhere [Sheridan et al., 1994]; thus only a brief description will be made here. Atmospheric particles were collected onto thin formvar films supported by transmission electron microscope (TEM) grids using a multiple-sample, low-pressure impactor system mounted onboard the NASA ER-2. The impactor was able to efficiently collect particles ranging from diameters >0.02 μm at cruise altitude to >0.06 μm at the surface. Up to 25 samples and blanks were collected during each flight at predetermined altitude levels or times, or during periods of interesting aerosol characteristics, with this system. Sampling duration was typically ~30 s, although this was adjustable if desired. The exposed grids were removed from their individual impactor cassettes in a nitrogen-purged glove box and placed in sealed storage containers. These samples were then shipped to our laboratory and stored in a low humidity environment until analysis.

Selection of samples for analysis was based primarily on location and altitude to ensure maximum latitudinal coverage for this study. In each analyzed sample, individual aerosol particles were characterized for size, morphology, and elemental composition using a 200-kV analytical transmission electron microscope equipped with an ultra-thin-window energy dispersive x-ray spectrometer at NIST in Boulder, Colorado. Particle counting, sizing, and classification was performed as described in Sheridan [1989] and Sheridan et al. [1994]. Five hundred particles were analyzed in all but one of the 61 selected samples, for a total of over 30,000 analyzed particles. Observations were made of particles in the central aerosol deposit (CAD) which was directly under the impactor jet. These CAD particles were not, however, included in the 500-particle statistics from each grid because the loadings in the CAD regions were often too high and particles were very close to or occasionally touching one another, compromising the individual composition analyses. Analysis was performed at several (at least three) randomly-chosen locations on the grid at increasing radial distances from the center of the deposit ranging from small (near the fringe of the CAD) to large (near the edge of the TEM grid). Since particle inertia effects in the circular jet may lead to size- or density-dependent distributions of particle types on the substrate [Rao et al., 1993; Sethi and John, 1993], we have employed this strategy to average out these potential sampling biases. This type of multiple-location analysis has been used by other researchers in the field to obtain more representative aerosol characterizations from single-jet impactors [e.g., Posfai et al., 1995]. Equal numbers of particles were analyzed in each analysis location. The substrate was moved slowly under high magnification such that particles were observed to pass through a rectangular box in the middle of the field-of-view (FOV). Any particles passing through the box were counted, sized, analyzed, and assigned a particle class, until a sufficient number of particles was observed in that location.

Our classification of thousands of particles as acidic and neutralized sulfate in previous works leads us to conclude that 1) sulfate is ubiquitous in the remote UT/LS, and 2) we know how sulfate appears and behaves under analysis conditions on our thin film substrates in our ATEM

[e.g., Sheridan, 1989; Sheridan et al., 1992, 1993, 1994]. All sulfate-class particles showed a round morphology, a similar image contrast with the film (implying a comparable density) in our imaging system, a comparable rate of volatilization or damage under the condensed electron beam, a strong S and weaker O signal, and many showed characteristic satellite droplets [Frank and Lodge, 1967; Bigg 1975; Ferek et al., 1983]. As mentioned earlier, sulfate particles may contain significant fractions of other species; there was however a major (> 50%) mass fraction of sulfate in particles classified as sulfate. Rather than expend considerable time and resources verifying that each droplet was in fact acidic sulfate, we confirmed ~10% of them by x-ray analysis. The fact that nearly all sulfate-class particles looked and behaved similarly under analysis and every confirmation x-ray spectrum showed the S and O peaks lead us to believe that we were classifying sulfate properly.

We did not attempt to determine sizes for particles classified as sulfate, because the observed sizes of sulfate particles in the ATEM do not accurately reflect their true atmospheric diameters due to spreading of the liquid on the thin film substrate [e.g., Gras and Ayers, 1979]. The thin disk or flattened hemispherical cap formed by the spreading acid has a diameter greater than that of the airborne particle that created it. Comparison of previous sulfate particle sizing studies [Frank and Lodge, 1967; Bigg and Ono, 1975; Gras and Ayers, 1979] shows large uncertainty (factor of several differences) in the estimation of pre-impaction diameters using the various models.

Since we know sulfate is a major constituent of the remote upper tropospheric and lower stratospheric aerosol and was dominant in our aerosol samples, we have focused on determining the types, relative amounts, and sizes of other interesting classes of particles. We have identified 4 macroclasses of nonsulfate particles, each consisting of several more-specific particle types. The macroclasses are carbon-rich (C-rich), crustal, metallic, and salts. Particles in the C-rich class show a dominant mass fraction of C, and may or may not have a chain aggregate morphology. The C-rich class contains carbon soot, particles that may be largely composed of organic C, and perhaps particles of intermediate compositions (soot/organic mixtures). Particles are classified as crustal if they contain major Si, or contain two or more of the common lithophilic elements Mg, Al, Ca, or Fe in a major mass fractions along with O. The metallic particle class contains particles containing metals such as Al, Ti, and Fe in major mass fractions, and metallic oxides. The salts class contains particles with major mass fractions of Na, K, Mg, or Ca, along with Cl and/or S. As discussed in Sheridan et al. [1994], the classification of a particle into a given class (such as crustal) does not imply knowledge of its source, merely that the particle's characteristics resemble particles typical of that class.

Principal Results

Laboratory test samples

Polystyrene latex (PSL) microspheres of various diameters were used to determine the minimum detectable particle size we could achieve using our electron microscope system. These microspheres were suspended in distilled water and placed in a nebulizer for aerosol generation. The aerosols were dried after generation and collected onto our thin-film impactor substrates for analysis. At our standard analysis magnification of 20,000x, 20-nm diameter microspheres were

clearly visible. The next smaller size microspheres (10 nm) were difficult to detect at 20,000x, although increasing the magnification to 50,000x permitted easy detection. This exercise demonstrated that a significant fraction of 10-nm particles could be missed in an analysis conducted at 20,000x, while the vast majority of 20-nm particles should be detected. Thus, our standard analysis procedures can not be considered valid for solid particles smaller than 0.02 μm. Liquid particles such as sulfuric acid show a lower contrast with the thin film substrate, and are thus more difficult to observe. The minimum detectable size for these particles was near 0.03 μm.

We confirmed from previous studies typical elemental detection limits with our EM system. For the NIST/Boulder STEM operating at 200 keV, detection limits for most elements above Na in 1 μm diameter particles were ~0.1% (by weight). As atomic number decreased, detection efficiency also decreased so that, for example, the C detection limit above the thin-film background contribution for 1-μm particles was around several percent. As particle size decreased, detection limits were higher, especially for the light elements. Particles composed largely of only a few elements, such as atmospheric sulfuric acid droplets, showed a S signal down to detected particle sizes of <0.1 μm. Since the acidic droplets spread out on several types of thin-film substrates, the true atmospheric sizes of these particles are somewhat smaller than their analyzed sizes (Gras and Ayers, 1979).

For particles containing a large mass fraction of elements that are efficiently detected by our x-ray spectrometer, the minimum particle size from which we could obtain elemental information was smaller than 0.1 μm. Fine particles containing Fe were generated by grinding Fe_2O_3 in a mill for long periods of time. Some particles in the resulting powder were smaller than 0.05 μm in size. A weak Fe signal was observed in particles as small as 0.05 μm, whereas smaller Fe-containing particles generally showed no detectable elements. This study suggests that very small particles containing large mass fractions of efficiently-detected elements (i.e., elements above Z = 12) should be detectable using our approach.

In earlier work, we studied the deposition pattern from our single-jet impactor. Typically, a central deposit of particles was evident, with lighter mass loadings of particles in areas away from the central deposit. A combination of two factors was working here; namely, the aerodynamic diameters of most generated particles being above the impactor cut point at the operating pressure and a slight focusing tendency for this particular impactor. The deposition patterns of single-jet impactors have been discussed in the literature (Rao et al., 1993; Sethi and John, 1993), and caution is necessary in interpreting results of this type. Specifically, the distribution of particles in the deposit of a circular jet impactor depends upon their aerodynamic diameters. Put another way, the collection efficiency for particles of different Stokes numbers varies as a function of radial distance from the center of the impactor jet. Thus the relative abundances of, for example, sulfate and non-sulfate particles in the air may differ from those observed at a given location on the collection substrate. We attempted to alleviate this potential problem by ramping up the flow through the impactor and then ramping it down at the completion of the sample. This should blur any preferential deposition location for specific particle types and essentially spread all types of particles over the entire substrate.

To determine whether particle type was a function of analysis location, different portions of the test substrates were inspected and any preferential deposition locations based on radial distance from the center of the particulate deposit noted. No major particle speciation based on particle composition was observed, although particle sizes were generally larger nearer to the center of the aerosol deposit. This was difficult to quantify for generated sulfuric acid particles, since many individual liquid droplets in the heavy deposit area may have coalesced to form fewer larger ones. The particle size gradation was, however, easily observed for solid test particles.

ASHOE/MAESA and Other Atmospheric Samples

Latitude-Altitude plots showing the number fractions of C-rich, crustal, metallic, and salts particles in our samples are shown in Figures 1-4. Most of these samples were collected over the Pacific Ocean, so the sampling longitude does not vary much with latitude. Inspection of the four graphs reveals that only infrequently did the number fraction of any of these particle macroclasses exceed 2% of the total analyzed particles. Particles composed mostly of sulfate typically dominated the particle numbers, typically exceeding 90% of all particles in remote upper troposphere/lower stratosphere aerosol samples. As discussed above, if a particle contained two major physical or chemical phases that could be assigned to different macroclasses, a determination of which phase constituted the majority of the particle was made and the particle was assigned to that class. The other major observed particle type that does not fall under sulfate or one of the macroclasses is "low counts", usually consisting of very small particles that do not have enough mass to be detected above instrument background. Low counts particles, if above ~0.05 μm in size, are thought to be C-rich, since a major mass fraction of heavier elements should be detected by our spectrometer. These results are presented in tabular form in Table 1.

C-rich particles (shown in Fig.1) are defined as having C as the major element (by mass) detectable using x-ray spectrometry. No morphological screening was performed in order to distinguish soot from other types of particles, as has been done in numerous earlier works [e.g., Sheridan et al., 1994; Pueschel et al., 1992; Blake and Kato, 1995]. Recent work by our group on jet aircraft exhaust emissions during the NASA SNIF-III program suggests that C-rich particles are emitted by aircraft over a wide range of morphologies, from roughly equidimensional to highly fractal chain aggregates, with elemental compositions and behaviors in the electron beam that are essentially identical. We chose not to attempt to classify soot based on morphology because of the likelihood that many non-fractal soot particles would be misidentified this way.

Nearly all tropospheric Northern Hemisphere samples showed elevated (>2% by number) amounts of C-rich particles, while only one of the Southern Hemisphere samples did. We acknowledge that these relatively few samples make the definitive determination of a gradient difficult. Still, the suggestion of a latitudinal gradient in tropospheric C-rich particles is there. Stratospheric C-rich particles do not show a latitudinal gradient at cruise altitude. It is clear, however, that larger number fractions of C-rich particles were consistently observed in tropospheric aerosol samples than in stratospheric samples. Figure 2 shows the analyses of aerosol samples for C-rich particles from the midlatitudes of both hemispheres. It is clear from this plot that the highest number fractions of C-rich particles are found in the troposphere, and that the

northern hemisphere and southern hemisphere troposphere populations are indeed different (significantly different at the 0.05 level).

In Figure 3, a tropospheric latitudinal gradient of crustal class particles is observed and the interhemispheric differences are consistent with the much larger continental area in the NH. Most stratospheric samples show very low crustal particle number fractions, although a few are above 0.02, especially in the Southern Hemisphere. Some of these stratospheric samples may have been influenced by volcanic aerosols from the Rabaul eruption in mid-1994. The number fractions for crustal particles may be low in most samples due to rapid settling of the numerous coarse-fraction terrestrial particles.

Figure 4 shows the latitude-altitude distribution for metallic particles. There is a clear vertical gradient in the atmosphere, with few particles composed mostly of metallic elements observed above the tropopause. Most of the metallic elements encountered in particles were Al, Ti, and Fe, with other metals less frequently observed. Again, a latitudinal gradient is difficult to determine because of the limited number of descents into the troposphere and the similarity of metallic number fractions in midlatitude samples from both hemispheres.

It appears that marine and other salt particles show a slight latitudinal gradient in Figure 5, with higher number fractions observed in the Southern Hemisphere. This is consistent with a greater fraction of area in the Southern Hemisphere covered by oceans. There does not appear to be a strong vertical gradient across the tropopause in either hemisphere. Samples of with higher salts number fractions were observed at higher altitudes in the Southern Hemisphere. This again could be debris from the eruption of the remote Southern Hemisphere volcano Rabaul.

At the request of our colleague, Prof. J.C. Wilson of the University of Denver, we undertook the analysis of 6 aerosol impactor samples from the 1995 NASA STRAT Airborne Field Deployment. The analysis of these samples was discussed as a possibility in our continuation proposal in 1995. Analysis of these samples revealed a compromised sampling system during the first STRAT deployment of October 1995; samples showed no central aerosol deposit which usually means that insufficient flow through the impactor, possibly due to a leak, was the case. All 6 of the analyzed STRAT samples showed this condition, so for now we conclude that all samples in the first STRAT mission were compromised. Analysis of samples from the second and later deployments showed normal particle deposition patterns, so the condition appears to have been corrected.

Use of the High-Resolution Field Emission Analytical Electron Microscope

On two different occasions we attempted to analyze (and also re-analyze) ASHOE/MAESA aerosol samples using the field-emission analytical electron microscope at NIST/Gaithersburg. In both cases, we determined that the newer instrument was actually inferior in performance to our older analytical electron microscope for the analysis of atmospheric particles. The new field-emission microscope provides an electron beam current density of roughly 10 times what conventional TEMs can. This is good for analyzing (i.e., obtaining high resolution images and compositional information from) very small, solid, stable particles. This higher beam power leads

to significantly higher temperatures in the particles, and volatilization and particle destruction result. Most atmospheric particles we analyzed using this new microscope underwent rapid and severe beam damage, so we conclude that this instrument used in this manner is not very useful for atmospheric particle analysis.

Conclusions

In general, the aerosol both above and below the tropopause was dominated by submicrometer liquid-phase sulfate particles. Non-sulfate particles were present in higher number fractions in the UT samples, although these particles rarely accounted for more than about 10% of the analyzed particles. The non-sulfate particles included solid particles containing common crustal elements, mixed-salt and marine salt particles, C-rich particles, and metallic particles. Most of the UT non-sulfate particles were externally mixed with the sulfate particles; i.e., no appreciable S coatings were observed on the vast majority of UT non-sulfate particles. Some composite particles were present in most samples; in these cases the particles were classified according to the major mass fraction. Finally, non-sulfate particles with possible aircraft sources such as C soot and metal-containing particles, were, when observed, overwhelmingly observed in the UT samples. This could reflect the fact that in the northern midlatitudes, the majority of commercial aircraft mileage is through the UT, or possibly a difference in emissions between subsonic and higher-flying supersonic aircraft. These soot and metal particles, while perhaps only a small number fraction of aircraft-emitted particles in the atmosphere, may be useful as tracers of aircraft activity, because the more numerous particulate aircraft emissions that promote sulfate formation may be indistinguishable from the background aerosol.

Extended Studies and Ongoing Research

We are currently conducting fundamental collection efficiency studies with the University of Denver's low-pressure impactor sampler to determine its collection efficiency for particles of different types and sizes. This is especially important given the disagreement in published abundances of soot and other particle types between our group and others. As soon as we determine the appropriate scaling factors, we will publish these data in a refereed journal.

Educational Opportunities

Three undergraduate students at the University of Colorado took part in the reduction of data from the electron microscope analysis. These were Sean Metrick, Brain Hagen, and Craig Morrison. These students were not supported directly through this grant, but rather through a student work-study program sponsored by the Colorado Commission for Higher Education (CCHE).

Presentations of These Data

Wilson, J.C., P.J. Sheridan, C.A. Brock, and D. Gesler, Composition and size distributions of upper tropospheric and lower stratospheric aerosol particles in 1993-1994, American Geophysical Union Fall Meeting, San Francisco, California, December 1997.

Wilson, J.C., D.W. Gesler, C.A. Brock, P.J. Sheridan, B.E. Anderson, and W.R. Cofer, Analysis of particles emitted by C-130 and F-16 aircraft and collected in SNIF-III, AEAP Annual Meeting, Virginia Beach, VA, May 1998.

References

Bigg, E.K., Size distributions of stratospheric aerosols and their variations with altitude and time, J. Atmos. Sci., 33, 1080-1086, 1976.

Bigg, E.K., and A. Ono, Size distribution and nature of stratospheric aerosols, paper presented at IAMAP/IAPSO Combined First Special Assembly, Melbourne, 1975.

Blake, D., and K. Kato, Latitudinal distribution of carbon soot in the upper troposphere and lower startosphere, J. Geophys. Res., 100, 7195-7202, 1995.

Bigg, E.K., Stratospheric particles, J. Atmos. Sci., 32, 910-917, 1975.

Ferek, R.J., A.L. Lazrus, and J.W. Winchester, Electron microscopy of acidic aerosols collected over the northeastern United States, Atmos. Environ., 17, 1545-1561, 1983.

Frank, E.R. and J.P. Lodge, Morphological identification of airborne particles with electron microscopy, J. Microscopy, 6, 449-456, 1967.

Gras, J.L. and G.P. Ayers, On sizing impacted sulfuric acid particles, J. Appl. Met., 18, 634-638, 1979.

Posfai, M., J.R. Anderson, P.R. Buseck, and H. Sievering, Compositional variations of sea-salt-mode aerosol particles from the North Atlantic, J. Geophys. Res., 100, 23063-23074, 1995.

Pueschel, R.F., D.F. Blake, K.G. Snetsinger, A.D.A. Hansen, S. Verma, and K. Kato, Black carbon (soot) aerosol in the lower stratosphere and upper troposphere, Geophys. Res. Lett., 19, 1659-1662, 1992.

Rao, N.P., J. Navascues and J. Fernandez de la Mora, Aerodynamic focusing of particles in viscous jets, J. Aerosol Sci., 24, 879-892, 1993.

Sethi, V. and W. John, Particle impaction patterns from a circular jet, Aerosol Sci. Technol., 18, 1-10, 1993.

Sheridan, P.J., Analytical electron microscope studies of size-segregated particles collected during AGASP-II, Flight 201-203, J. Atmos. Chem., 9, 267-282, 1989.

Sheridan, P.J., R.C. Schnell, D.J. Hofmann, J.M. Harris, and T. Deshler, Electron microscope studies of aerosol layers with likely Kuwaiti origins over Laramie, Wyoming during spring 1991, Geophys. Res. Lett., 19, 389-392, 1992

Sheridan, P.J., R.C. Schnell, J.D. Kahl, J.F. Boatman, and D.M. Garvey, Microanalysis of the aerosol collected over south-central New Mexico during the ALIVE field experiment, May-December, 1989, Atmos. Environ., 27A, 1169-1183, 1993.

Sheridan, P.J., C.A. Brock and J.C. Wilson, Aerosol particles in the upper troposphere and lower stratosphere: Elemental composition and morphology of individual particles in northern midlatitudes, Geophys. Res. Lett., 21, #23, 2587-2590, 1994.

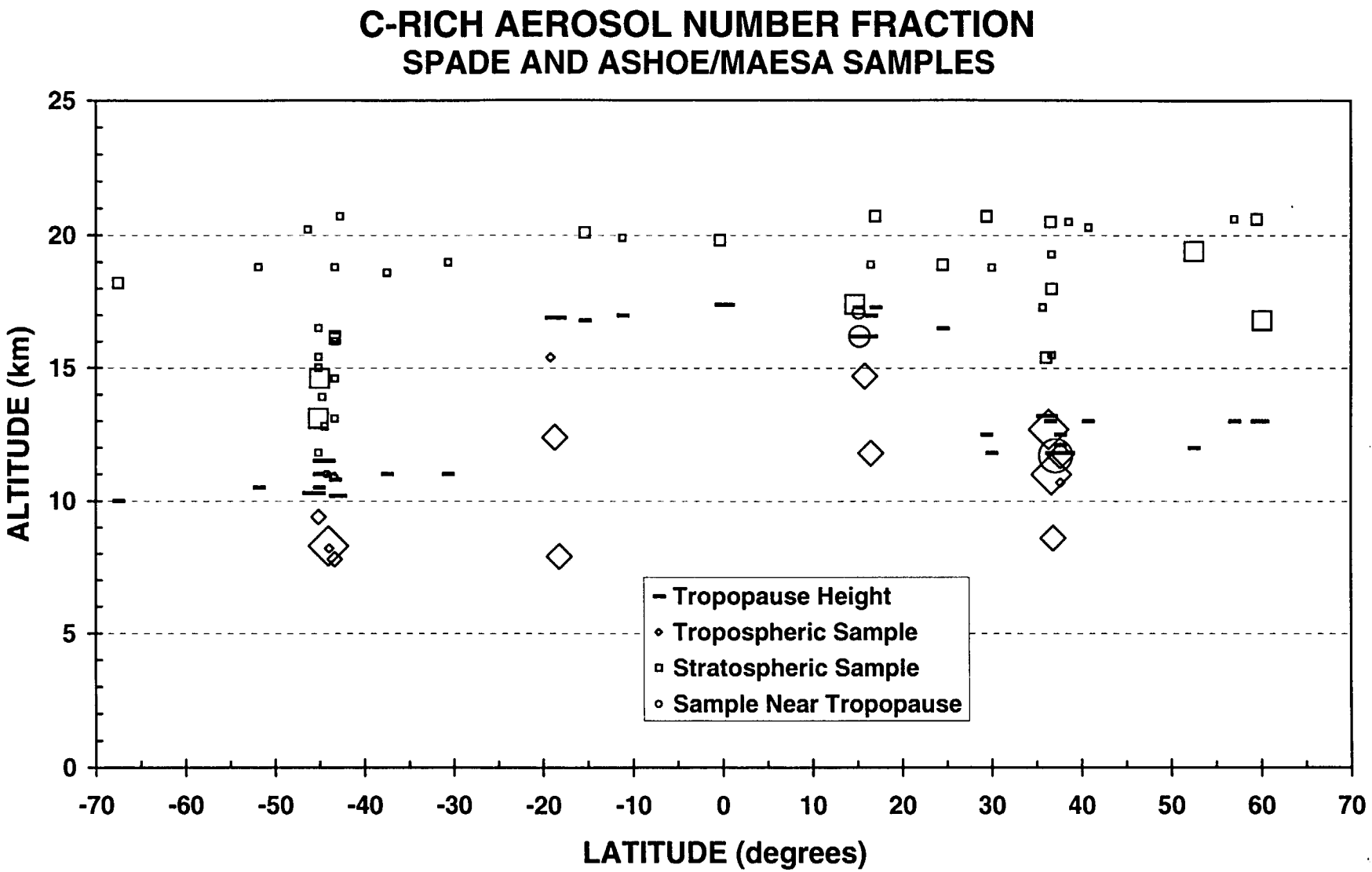
C-RICH AEROSOL NUMBER FRACTION
SPADE AND ASHOE/MAESA SAMPLES
ALTITUDE (km)
25
20
15
10
5
0
-70
-60
-50
-40
-30
-20
-10
0
10
20
30
40
50
60
70
LATITUDE (degrees)
Tropopause Height
Tropospheric Sample
Stratospheric Sample
Sample Near Tropopause
Symbol Size: 1 = NF<0.005, 2 = 0.005<NF<0.01, 3 = 0.01<NF<0.02, 4 = NF>0.02

Fig. 1

Northern Midlatitudes vs Southern Midlatitudes
C-Rich Particles

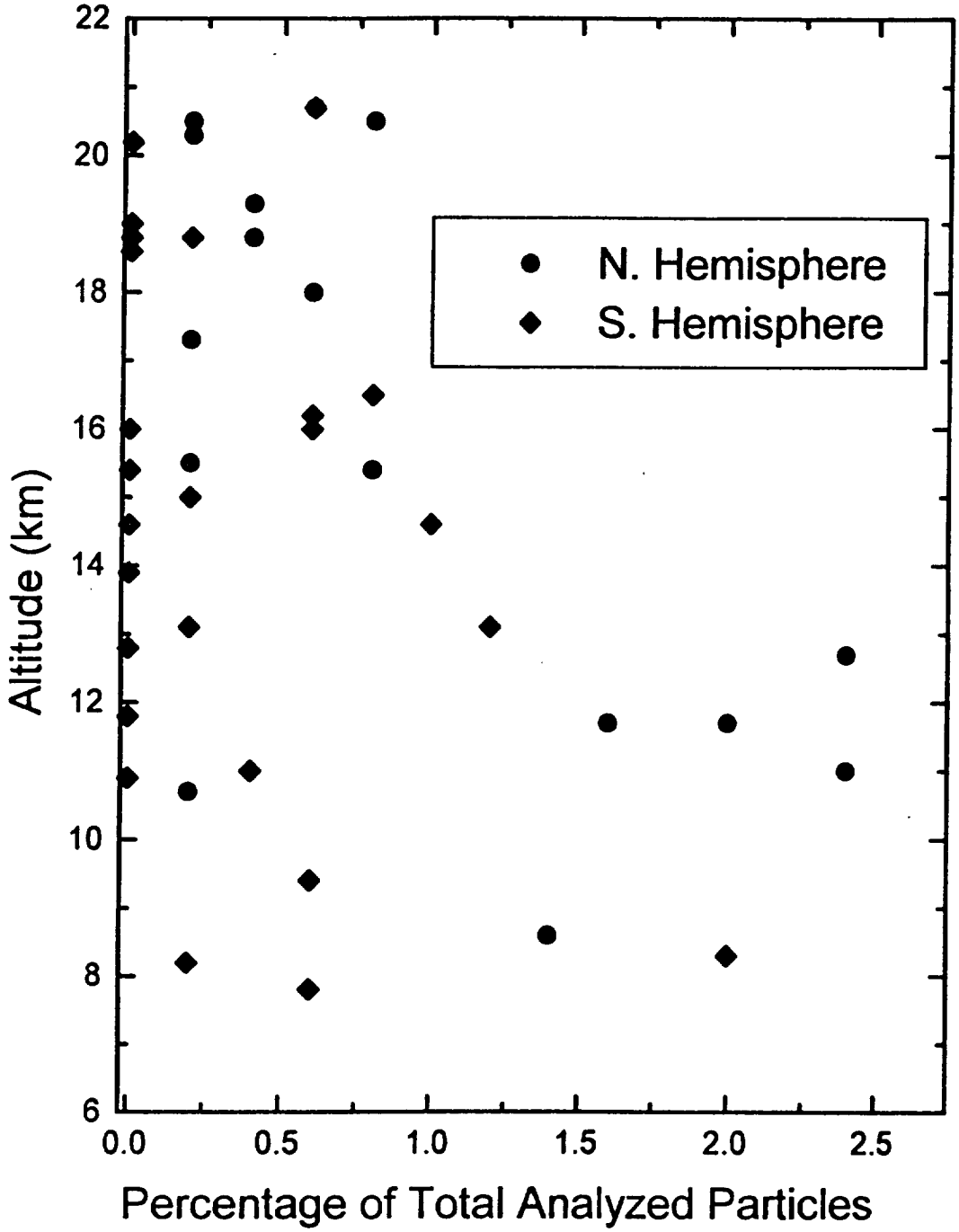

In the troposphere (below about 12 km), the two populations are significantly different at the 0.05 level.

Fig. 2

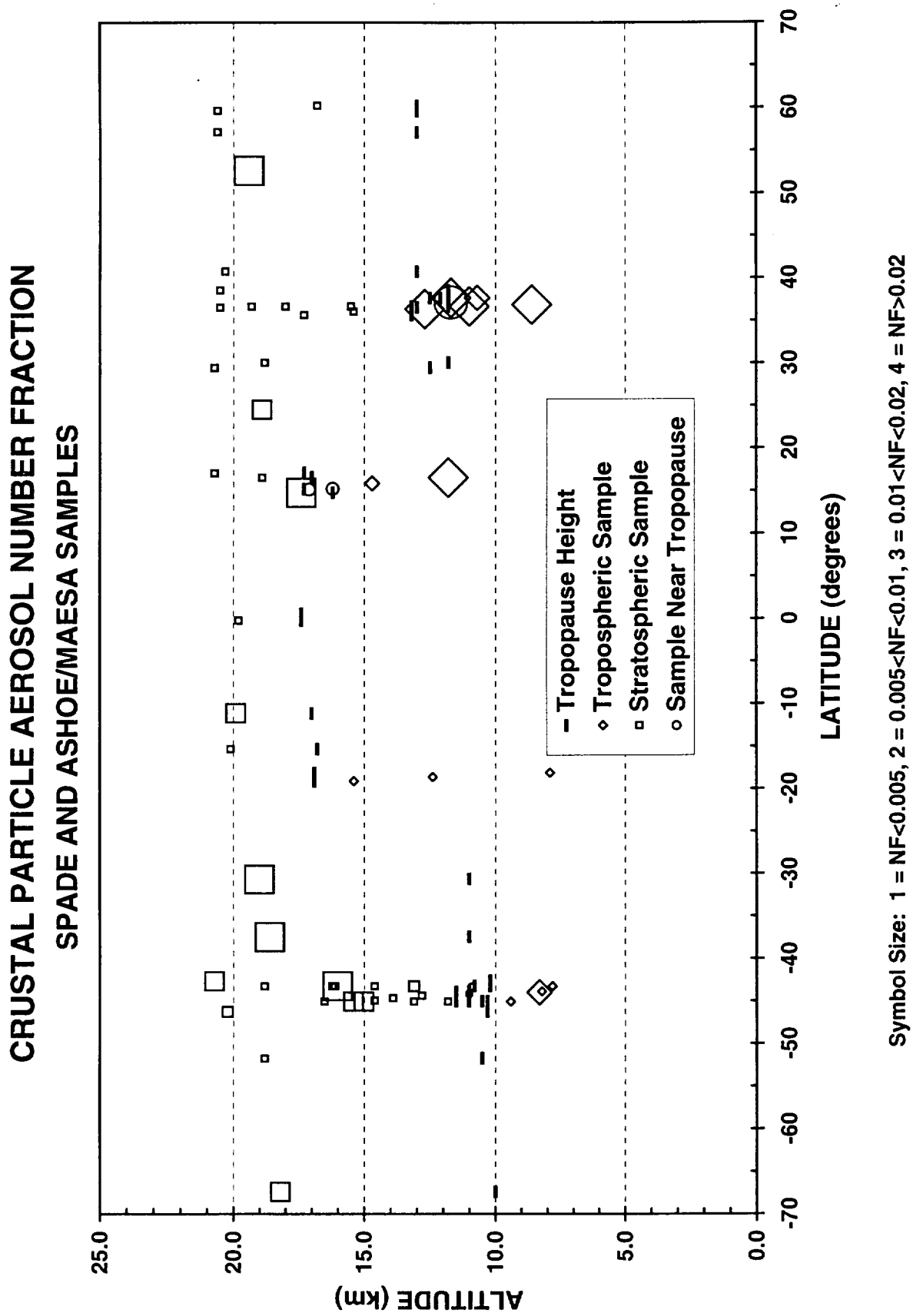
CRUSTAL PARTICLE AEROSOL NUMBER FRACTION
SPADE AND ASHOE/MAESA SAMPLES
ALTITUDE (km)
25.0
20.0
15.0
10.0
5.0
0.0
LATITUDE (degrees)
-70
-60
-50
-40
-30
-20
-10
0
10
20
30
40
50
60
70
Tropopause Height
Tropospheric Sample
Stratospheric Sample
Sample Near Tropopause
Symbol Size: 1 = NF<0.005, 2 = 0.005<NF<0.01, 3 = 0.01<NF<0.02, 4 = NF>0.02

Fig. 3

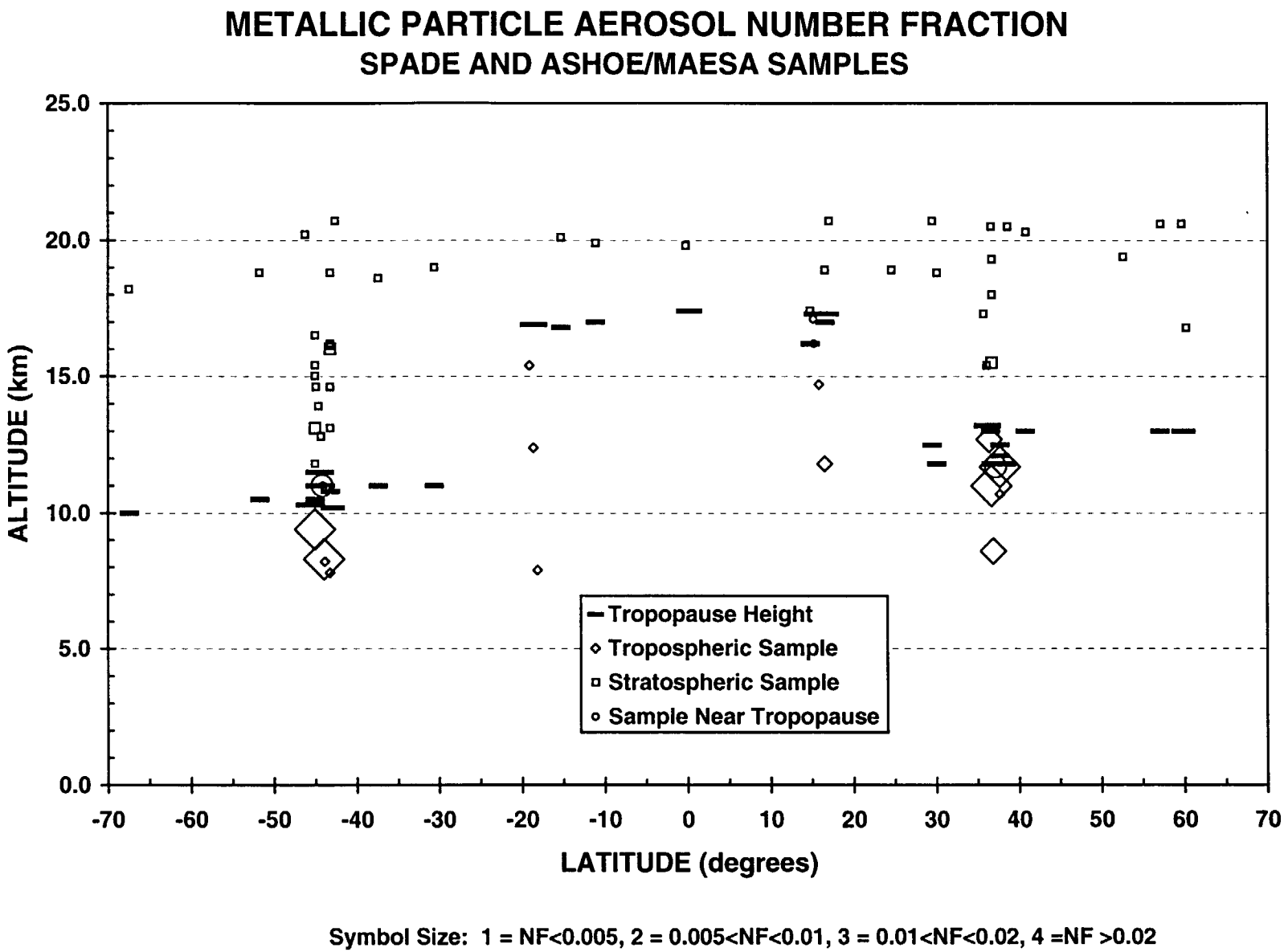
METALLIC PARTICLE AEROSOL NUMBER FRACTION
SPADE AND ASHOE/MAESA SAMPLES
ALTITUDE (km)
25.0
20.0
15.0
10.0
5.0
0.0
-70
-60
-50
-40
-30
-20
-10
0
10
20
30
40
50
60
70
LATITUDE (degrees)
Tropopause Height
Tropospheric Sample
Stratospheric Sample
Sample Near Tropopause
Symbol Size: 1 = NF<0.005, 2 = 0.005<NF<0.01, 3 = 0.01<NF<0.02, 4 =NF >0.02

Fig. 4

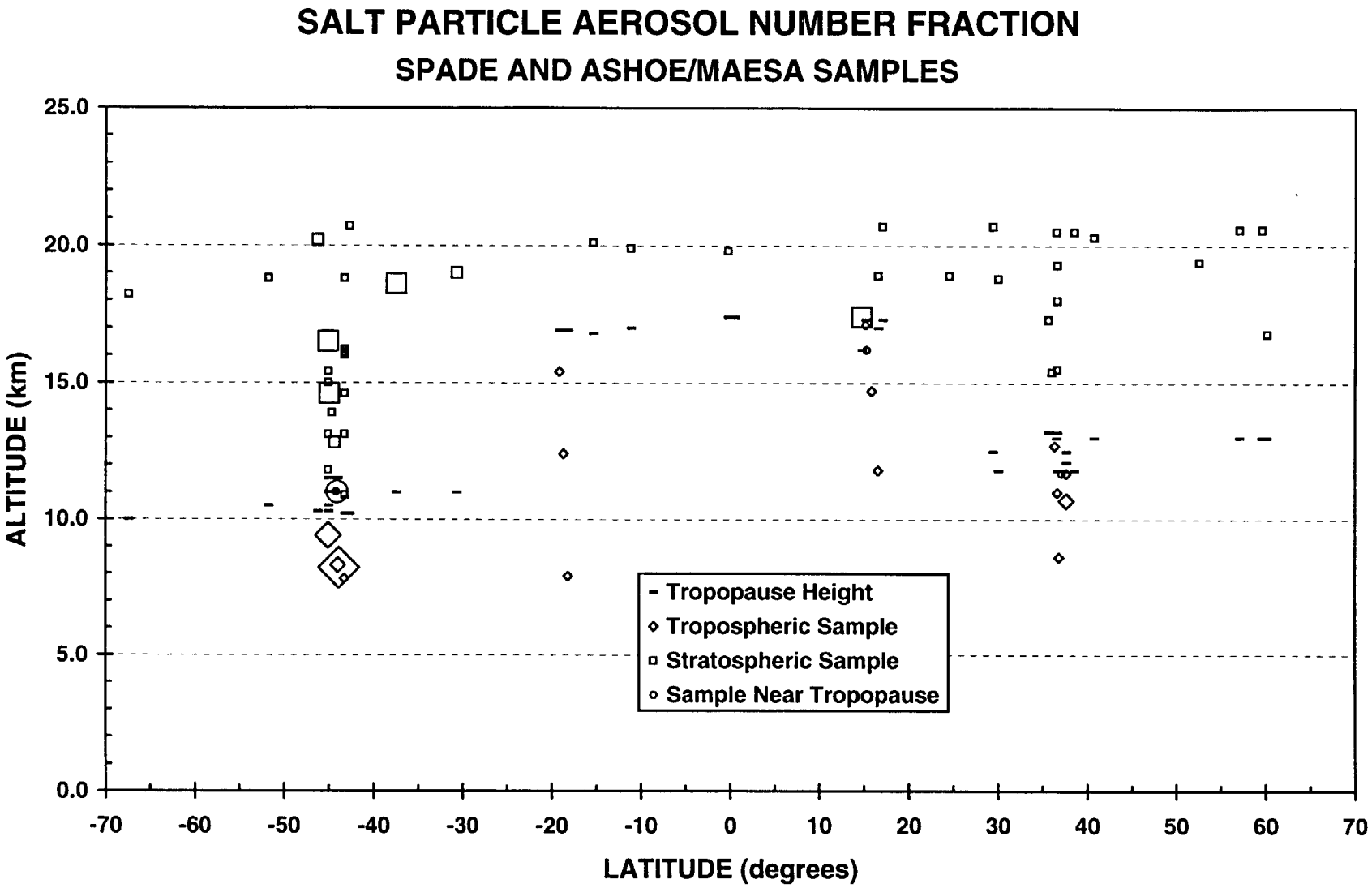
SALT PARTICLE AEROSOL NUMBER FRACTION
SPADE AND ASHOE/MAESA SAMPLES
ALTITUDE (km)
25.0
20.0
15.0
10.0
5.0
0.0
-70
-60
-50
-40
-30
-20
-10
0
10
20
30
40
50
60
70
LATITUDE (degrees)
Tropopause Height
Tropospheric Sample
Stratospheric Sample
Sample Near Tropopause
Symbol Size: 1 = NF<0.005, 2 = 0.005<NF<0.01, 3 = 0.01<NF<0.02, 4 = NF>0.02

Fig. 5

Table 1

Sample#	Latitude	Altitude (km)	Strat/ Trop	Counted Particles	C-Rich Particles	Crustal Particles	Metallic Particles	Salt Particles	C-rich Particle # Fraction	Crustal Particle # Fraction	Metallic Particle # Fraction	Salt Particle # Fraction	Total Nonsulfate # Fraction
930501_3	40.8	20.3	S	500	1	2	0	0	0.002	0.004	0.000	0.000	0.006
930501_10	57.1	20.6	S	500	2	0	1	0	0.004	0.000	0.002	0.000	0.006
930501_11	59.6	20.6	S	500	4	1	1	0	0.008	0.002	0.002	0.000	0.012
930501_12	60.2	16.8	S	500	6	3	2	1	0.012	0.006	0.004	0.002	0.024
930503_5	30.1	18.8	S	500	2	1	1	2	0.004	0.002	0.002	0.004	0.012
930503_7	16.6	18.9	S	500	1	1	0	0	0.002	0.002	0.000	0.000	0.004
930506_2	37.7	11.7	T	500	8	13	10	0	0.016	0.026	0.020	0.000	0.062
930506_9	36.6	20.5	S	500	4	0	0	1	0.008	0.000	0.000	0.002	0.010
930506_15	35.7	17.3	S	278	1	2	0	0	0.004	0.007	0.000	0.000	0.011
930506_16	36.1	15.4	S	500	4	4	0	0	0.008	0.008	0.000	0.000	0.016
930506_17	36.4	12.7	T	500	12	14	8	2	0.024	0.028	0.016	0.004	0.072
930506_18	36.7	11.0	T	500	12	21	12	2	0.024	0.042	0.024	0.004	0.094
930512_13	38.6	20.5	S	500	1	3	0	1	0.002	0.006	0.000	0.002	0.010
930512_17	36.7	19.3	S	500	2	4	2	0	0.004	0.008	0.004	0.000	0.016
930512_18	36.7	18.0	S	500	3	9	1	0	0.006	0.018	0.002	0.000	0.026
930512_19	36.7	15.5	S	500	1	4	3	0	0.002	0.008	0.006	0.000	0.016
930512_20	37.2	11.7	T/S	500	10	25	8	2	0.020	0.050	0.016	0.004	0.090
930512_21	36.9	8.6	T	500	7	18	5	1	0.014	0.036	0.010	0.002	0.062
930514_2	37.7	10.7	T	500	1	6	1	4	0.002	0.012	0.002	0.008	0.024
930514_10	29.5	20.7	S	500	3	5	1	1	0.006	0.010	0.002	0.002	0.020
930514_12	17.1	20.7	S	500	4	9	0	0	0.008	0.018	0.000	0.000	0.026
930514_14	15.2	17.1	T/S	500	4	3	1	1	0.008	0.006	0.002	0.002	0.018
940321_9	-0.2	19.8	S	500	3	0	1	2	0.006	0.000	0.002	0.004	0.012
940321_11	0.6	15.7	T	no counts									
940327_9	-15.3	20.1	S	500	3	1	0	2	0.006	0.002	0.000	0.004	0.012
940329_1	-18.1	7.9	T	500	9	0	0	0	0.018	0.000	0.000	0.000	0.018
940329_2	-18.6	12.4	T	500	6	0	0	0	0.012	0.000	0.000	0.000	0.012
940329_3	-19.1	15.4	T	500	2	2	0	0	0.004	0.004	0.000	0.000	0.008
940408_1	-43.9	8.3	T	500	10	5	26	3	0.020	0.010	0.052	0.006	0.088
940408_2	-44.1	11.0	T/S	500	2	2	5	0	0.004	0.004	0.010	0.000	0.018
940408_4	-44.9	14.6	S	500	5	11	0	5	0.010	0.022	0.000	0.010	0.042
940408_17	-45.0	16.5	S	500	4	5	0	6	0.008	0.010	0.000	0.012	0.030
940408_18	-45.0	13.1	S	500	6	5	3	0	0.012	0.010	0.006	0.000	0.028
940408_19	-45.0	9.4	T	500	3	2	17	5	0.006	0.004	0.034	0.010	0.054
940523_4	-43.2	16.0	S	500	3	10	4	4	0.006	0.020	0.008	0.008	0.042
940523_5	-42.6	20.7	S	500	3	6	1	2	0.006	0.012	0.002	0.004	0.024
940528_1	-43.2	7.8	T	500	3	2	2	2	0.006	0.004	0.004	0.004	0.018
940528_2	-43.2	10.9	T/S	500	0	0	0	0	0.000	0.000	0.000	0.000	0.000
940528_3	-43.2	13.1	S	500	1	3	0	1	0.002	0.006	0.000	0.002	0.010
940528_4	-43.2	14.6	S	500	0	0	0	0	0.000	0.000	0.000	0.000	0.000
940528_6	-43.2	16.0	S	500	0	0	0	0	0.000	0.000	0.000	0.000	0.000
940528_7	-43.2	18.8	S	500	0	1	0	0	0.000	0.002	0.000	0.000	0.002
940528_14	-43.2	16.2	S	500	3	0	0	0	0.006	0.000	0.000	0.000	0.006
940603_5	-45.0	15.4	S	500	0	6	1	0	0.000	0.012	0.002	0.000	0.014
940603_7	-51.7	18.8	S	500	1	1	0	1	0.002	0.002	0.000	0.002	0.006
940806_15	-46.2	20.2	S	500	0	3	0	3	0.000	0.006	0.000	0.006	0.012
940806_16	-45.0	11.8	S	500	0	1	0	1	0.000	0.002	0.000	0.002	0.004
941016_1	-43.8	8.2	T	500	1	1	0	15	0.002	0.002	0.000	0.030	0.034
941016_2	-44.0	11.0	T/S	500	2	0	0	8	0.004	0.000	0.000	0.016	0.020
941016_3	-44.3	12.8	S	500	0	1	1	4	0.000	0.002	0.002	0.008	0.012
941016_4	-44.6	13.9	S	500	0	0	0	0	0.000	0.000	0.000	0.000	0.000
941016_5	-45.0	15.0	S	500	1	7	2	1	0.002	0.014	0.004	0.002	0.022
941016_10	-67.4	18.2	S	500	4	9	1	0	0.008	0.018	0.002	0.000	0.028
941024_1	-37.4	18.6	S	500	0	17	0	6	0.000	0.034	0.000	0.012	0.046
941024_2	-30.6	19.0	S	500	0	11	0	3	0.000	0.022	0.000	0.006	0.028
941024_5	-11.1	19.9	S	500	0	8	2	0	0.000	0.016	0.004	0.000	0.020
941024_9	14.8	17.4	T/S	500	6	29	1	5	0.012	0.058	0.002	0.010	0.082
941024_10	15.3	16.2	T	500	8	3	2	2	0.016	0.006	0.004	0.004	0.030
941024_11	15.9	14.7	T	500	6	4	1	0	0.012	0.008	0.002	0.000	0.022
941024_13	16.6	11.8	T	500	5	11	3	1	0.010	0.022	0.006	0.002	0.040
941102_6	24.6	18.9	S	500	3	8	2	0	0.006	0.016	0.004	0.000	0.026
941104_18	52.6	19.4	S	500	5	14	3	1	0.010	0.028	0.006	0.002	0.046